Phase Separation Behavior of Poly(vinyl alcohol) Solutions in Relation to the Drawability of Films Prepared from the Solutions

Masaru Matsuo,* Mutsuko Kawase, Yuri Sugiura, Satomi Takematsu, and Chisako Hara

Department of Clothing Science, Faculty of Home Economics, Nara Women's University Nara 630, Japan

Received April 6, 1992; Revised Manuscript Received March 26, 1993

ABSTRACT: Phase separation in solutions of poly(vinyl alcohol) in dimethyl sulfoxide/water mixtures was investigated by elastic and inelastic light scattering. In the initial stage of phase separation, a plot of the logarithm of scattered intensity against time exhibited a straight line described within the framework of a linearized spinodal decomposition theory by Cahn. Nevertheless, the scattering vector at the maximum value of the relaxation rate shifted to lower temperature on increasing the difference between the experimental temperature and the spinodal temperature, indicating inconsistency with the theory proposed by van Aartsen for spinodal decomposition of polymer solutions. Furthermore, the diffusion coefficient estimated by inelastic light scattering decreased in the range of time scale where linear plots of the logarithm of the scattered intensity against time were obtained. Accordingly, it can be concluded that even in the initial stage of phase separation, spinodal decomposition and gelation occur simultaneously. Thus, the phase separation of the PVA solutions is quite different from spinodal decomposition of amorphous polymer solutions and liquid–liquid phase separation of amorphous polymer blends, as has been reported generally. The occurrence of spinodal decomposition was found to hamper facile drawability of dried gel films prepared from the poly(vinyl alcohol) solutions.

Introduction

Poly(vinyl alcohol) (PVA) is a well-known polymer whose crystal lattice modulus measured by the X-ray diffraction technique is close to that of polyethylene. An attempt to improve the Young's modulus has been made but the value was much lower than the crystal lattice modulus in spite of a molecular structure similar to that of polyethylene. Recently, Hyon et al. succeeded in producing high-modulus PVA films by drawing of gels prepared by crystallization from semidilute solutions in water (H_2O) and dimethyl sulfoxide (Me_2SO) mixtures, the content of Me_2SO as cosolvent being 70 vol %.[3] Their method is based on a report by Friedberg et al. that solvent mixtures ranging from 50 to 70 vol % Me_2SO do not freeze at −100 °C because of hydration.[4] On the basis of the results of Hyon et al.,[3] the drawability of PVA gel films was studied as a function of degree of polymerization, cosolvent composition, concentration of solution, and quenching temperature of solution in a series of preliminary experiments reported elsewhere.[5] It was found that the cosolvent composition and the quenching temperature of the solutions have a significant effect on the drawability of dried gel films obtained from the solutions, and the drawability is more pronounced as the crystallinity of the films decreases. Furthermore, the crystallinity of the films decreased at lower gelation temperatures, and this tendency was most marked for the specimen prepared from a solution with Me_2SO/H_2O mixtures with a composition 70/30 by volume.

Close observations revealed that the dried gel films prepared from mixed solvent solutions with the 70/30 composition which showed facile drawability are generally more transparent than films prepared from solutions with other compositions, and the transparency was more pronounced as the gelation temperature decreased. This phenomenon is thought to be due to the relative rates of phase separation and gelation. In this regard, it is crucial to understand the effect of the characteristics of PVA molecules in solution on the drawability of the resultant films.

The dynamics of the sol–gel transition of PVA has been investigated by Komatsu et al.[6] using the elastic light scattering technique for aqueous solutions. They pointed out that this system has a phase diagram in which the spinodal curve crosses the sol–gel transition curve as predicted by Coniglio et al. in relation to the site-bond correlated percolation problem.[7]

On the other hand, Fang and Brown obtained interesting results concerning the decay time distribution of permanent PVA gels prepared from narrow molecular weight distribution polymer by cross-linking using glutaraldehyde and the corresponding semidilute solutions.[8] They found two relaxation modes for the PVA solutions. They pointed out that the fast relaxation characterizes the diffusive motions in the transient gel formed by intrapenetration of molecular domains, while the slow mode is due to clusters and/or groups of chains having a size depending mainly on concentration and only slightly on temperature. Furthermore, in their experiment, the slow mode disappeared on formation of the permanent gels.

This paper deals with the kinetics of the phase separation in PVA solutions prepared from a cosolvent of Me_2SO and H_2O. The aim of this work is not only to study drawability of dried gel films prepared from the solutions in terms of characteristics of molecular chains in solution but also to study phase separation in solutions of crystalline polymers in comparison with phase separation of noncrystalline polymer solutions[9] and liquid–liquid phase separation of amorphous polymer blends.[10]

The decay rate of the scattered light intensity was measured by inelastic light scattering[11–13] to investigate the diffusion of molecular chains in solution based on the correlation function of the light scattered due to density fluctuations during spinodal decomposition and gelation. The translational diffusion coefficient of molecules defined on the basis of linearity between the decay rate and the square of the scattering vector is discussed in relation to the apparent diffusion coefficient associated with the spinodal decomposition.

* To whom correspondence should be addressed.

0024-9297/93/2226-4461$04.00/0

Experimental Section

PVA powder was used: the degree of polymerization was 2000 and the degree of hydrolysis was 98%. The ratio $\bar{M}_w/\bar{M}_n$ ($\bar{M}_w$ is the weight-average molecular weight and $\bar{M}_n$ is the number-average molecular weight) was estimated to be 3.20 by gel permeation chromatography. Mixtures of Me_2SO and H_2O were used as cosolvent, and when the content of Me_2SO in the mixed solvent was 70 vol %, the cosolvent was designated as the 70/30 composition. In the present experiments, two different cosolvents with compositions of 70/30 and 50/50 were used. The solutions were prepared by heating the well-blended polymer/solvent mixture at 105 °C for 40 min and the solution was quenched in a water bath at constant temperature. After standing for 5 days in the water bath at a constant temperature, the test tube containing the solutions was tilted. When the meniscus deformed but the specimen did not flow under its own weight, we judged that the solution had gelled. The lowest temperature at which the onset of gelation occurred within 5 days was defined as the gelation temperature. This is similar to the method used by Komatsu et al.[6]

The time-dependence of scattered intensity was measured by the elastic light scattering technique using a 6328-Å He–Ne laser (DLS-700 produced by Ohtsuka Electrics Co. Ltd.). Before the sample solution tube was placed into the light scattering apparatus, the solution was precooled by dipping into a di-*n*-butyl phthalate bath kept at 40 °C for 10 min. When the precooled solution tube was put into a thermoregulated di-*n*-butyl phthalate bath in the light scattering apparatus, it underwent a temperature drop to the desired temperature. The precooling was done to avoid convection of fluid by the extremely rapid temperature drop. The change in angular distribution of scattered intensity with time was measured during the isothermal phase separation process of the solution.

Photon correlation measurements were done by using an inelastic light scattering instrument (DLS-700 produced by Ohtsuka Electrics Co. Ltd.), which was constructed on the basis of a block diagram similar to that proposed by Nemoto et al.[14] In this instrument, a time interval digitizer (TI method) was employed as the photon counting method by generating a clock pulse whose frequency covers a fairly wide range from 100 MHz to 125 Hz. A 2K-word RAM (DMA) and an address counter were connected to the digitizer. Digitized data of the time intervals between neighboring pulses in an input pulse train were stored first in the RAM by addressing from 1 to 4096 and then transferred to the computer for counting the number $T(i)$ of all possible pairs of pulses whose time intervals were i and then storing these data in the ith channel. The adaptation of the DMA reduced the dead time to as little as 310 ns, thus enabling accurate measurements of decay rates at scattering angles up to 150°. In doing so, the method to measure the normalized autocorrelation function $g^2(\tau)$ is given by

$$g^2(\tau) = \frac{\langle G(i)\rangle}{\{4095/\sum_{i=1}^{4095} T(i)\}^2 \sum_{i=1}^{4095}\{T(i)-i\}} \quad (1)$$

where $G(i)$ is a measured autocorrelation function.

Elastic light scattering measurements were also carried out to measure the correlation distance and the mean radius of gyration in PVA solutions by using the same light scattering instrument (DLS-700 of Ohtsuka Electric Co. Ltd.). All solutions and solvents were clarified by means of ultrafiltration through solvent-resistant Durapore membranes (obtained from Millipore Filter Corp.) with a mean pore size of 0.1 ~ 0.8 μm. The pore size was selected by the concentration of the solution. The cell was carefully washed with heated ethanol and then dried in a special box constructed to avoid dust.

Results and Discussion

Figures 1 and 2 show the change in the logarithm of the scattered intensity as a function of time at various q observed for (1% w/w PVA solutions with the 50/50 and 70/30 compositions, where q, the magnitude of the scattering vector, is given by $q = (4\pi/\lambda)\sin(\theta/2)$, λ and θ being the wavelength of light in solution and the

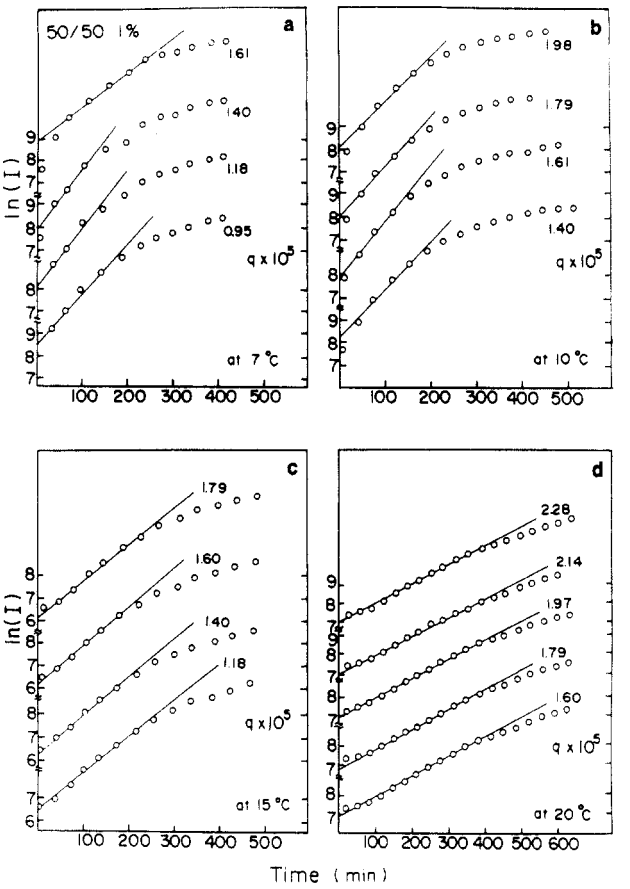

Figure 1. Change of the logarithm of the scattered intensity against time at various q measured for 1% w/w PVA solution with the 50/50 composition at various temperatures: (a) 7 °C; (b) 10 °C; (c) 15 °C; (d) 20 °C.

scattering angle, respectively. The temperature dependence of the refractive index could be neglected within the experimental error in the given temperature range. In the initial stage of phase separation, the logarithm of the scattered intensity increases linearly with time. The change in elastic scattered intensity in Figures 1 and 2 can be apparently described by the linear theory of spinodal decomposition proposed by Cahn,[15] which is given by

$$I(q,t) = I(q,t=0)\exp[2R(q)t] \quad (2)$$

where $I(q,t)$ is the scattered intensity at the time, t, after initiation of the spinodal decomposition, and $R(q)$ is the growth rate of concentration fluctuation given as a function of q; $R(q)$ is given by

$$R(q) = -D_c q^2\left\{\frac{\partial^2 f}{\partial c^2} + 2\kappa q^2\right\} \quad (3)$$

where D_c is the translational diffusion coefficient of the molecules in solution, f is the free energy of mixing, c is the concentration of solution, and κ is the concentration-gradient energy coefficient defined by Cahn and Hilliard.[16] A linear relationship in the plot of $\ln(I)$ vs t at fixed q was also obtained for solutions of other concentrations at various temperatures. According to the linear theory described by eqs 2 and 3, a plot of $\ln(I)$ vs t at fixed q should yield a straight line of slope $2R(q)$. With time, the logarithm of scattered intensity tends to deviate from the linear relationship, as has been calculated for the later stage of spinodal decomposition.[17-18] The deviation occurred for the solution with the 50/50 composition at shorter time scale in comparison with that at the 70/30 composition. Furthermore, although the results are not shown as figures in this paper, it was confirmed that the deviation shifts to shorter time scale with increasing

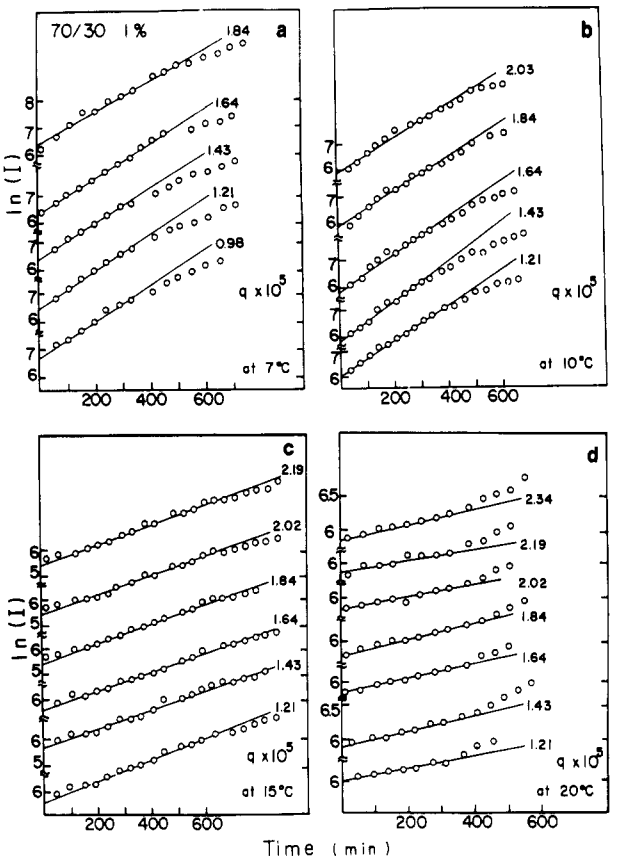

Figure 2. Change of the logarithm of the scattered intensity against time at various q measured for 1% w/w PVA solution with the 70/30 composition at various temperatures: (a) 7 °C; (b) 10 °C; (c) 15 °C; (d) 20 °C.

concentration of the solution, and this tendency is more pronounced in the case of the 50/50 composition. This indicates that the growth rate of concentration fluctuations is sensitive to the Me_2SO/H_2O composition.

The left-hand side of Figure 3 shows plots of $R(q)/q^2$ vs q^2 based upon the linear theory, which are obtained for the solutions with the 50/50 composition. A good linear relationship was obtained experimentally, indicating that the initial stage of the phase separation can be described within the framework of the linear theory. The apparent diffusion coefficient D_{app}, defined by $D_{app} = -D_c(\partial^2 f/\partial c^2)$, is given by the intercept on the vertical axis.

The right-hand side of Figure 3 shows the temperature dependence of D_{app} for solutions with the indicated concentrations at cosolvent compositions of 50/50. From the intercept on the temperature axis, one can estimate the spinodal temperature T_s, at which D_{app} is zero. Table I lists the spinodal temperature measured for the 50/50 and 70/30 compositions. The spinodal temperature T_s shifts to higher values as the concentration of solution increases, and this tendency is more pronounced in the case of the 50/50 composition. This indicates that the phase separation at the 50/50 composition is more significant than that at the 70/30 composition when both solutions have the same concentration.

Figure 4 shows plots of T_s vs concentration (points), while the curves show the concentration dependence of gelation temperature for data corresponding to the 50/50 composition (dashed curves) and the 70/30 composition (solid curve). At temperatures above the curves, the sol–gel transition cannot occur. At temperatures below the curves, the gelation rate became faster as temperature decreased. Here it may be noted that the gelation temperature is slightly higher than the spinodal temperature in the given concentration range. This indicates

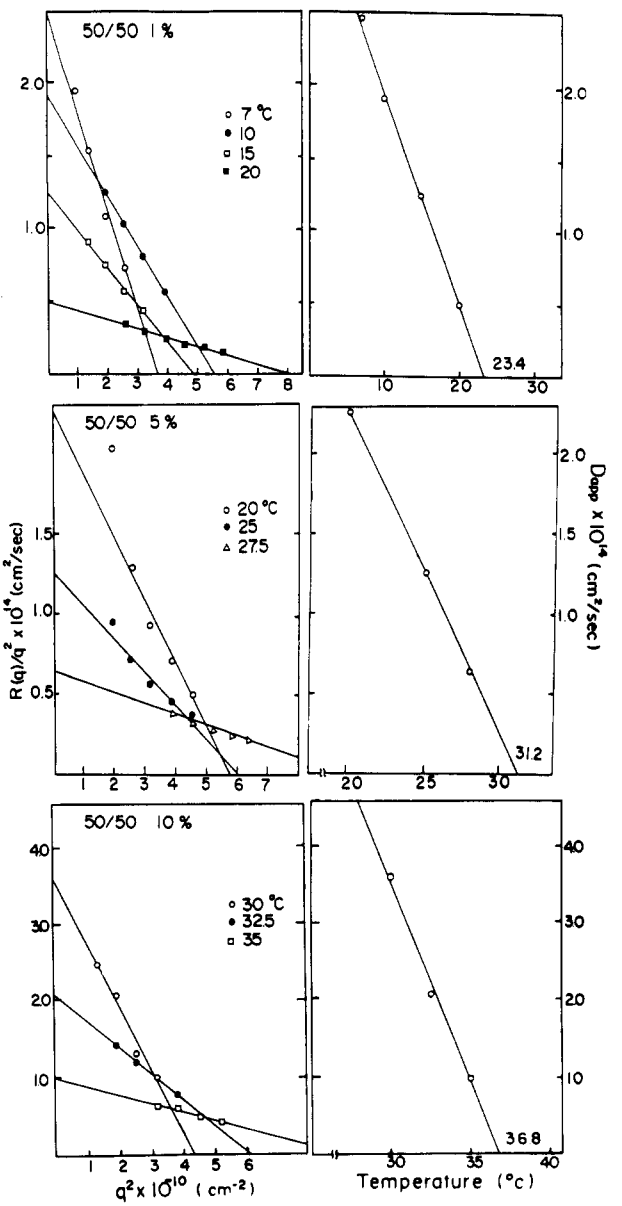

Figure 3. Left: Plots of $R(q)/q^2$ vs q^2 for PVA solutions with the 50/50 composition having the indicated concentrations. Right: Temperature dependence of the apparent diffusion coefficient D_{app}.

Table I. Spinodal Temperature (°C) of PBA Solutions at the Indicated Concentration for the 50/50 and 70/30 Compositions

	concn		
comp	1%	5%	10%
50/50	23.4	31.2	36.8
70/30	20.7	30.0	34.6

that both gelation and spinodal decomposition occur simultaneously, and this tendency is quite different from the phase diagram of aqueous solutions of PVA as reported by Komatsu et al.[6] According to these authors, the spinodal points and sol–gel transition curves divided the phase diagram into four regions: (i) a homogeneous sol region, (ii) a sol region under the spinodal curve indicating only spinodal decomposition, (iii) a gel region under the spinodal curve indicating simultaneous advance of both gelation and spinodal decomposition, and (iv) a gel region above the spinodal line, independent of liquid–liquid separation. In the present work, region ii could not be observed and the region iv in the cited work existed only in a very narrow temperature region as shown in Figure 4. The major part of Figure 4 corresponds to region iii. Actually, because of the simultaneous progression of

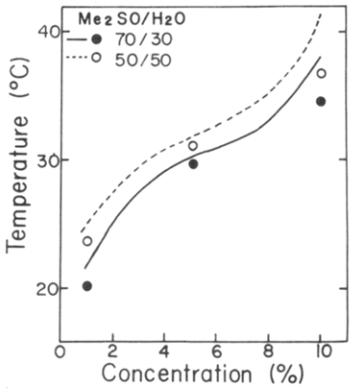

Figure 4. Plots: Spinodal temperature T_s vs concentration. Curves: Gelation temperature vs concentration for the 50/50 composition (dashed curve) and for the 70/30 composition (solid curve).

gelation and spinodal decomposition, it was impossible to observe a definite scattering peak as a function of q characterizing the later stage of spinodal decomposition, as has been reported for certain blend systems.[19]

To obtain more detailed information on the simultaneous progression of gelation and spinodal decomposition, light scattering patterns under the H_v polarization condition were observed as a function of time. Figures 5 and 6 show the results obtained for a 5% w/w solution at 20 °C and a 10% w/w solution at 30 °C, respectively. The logarithmic plots of scattered intensity at $\theta = 90°$ as a function of time are presented as a reference. In the time scale showing a straight line in the plot of $\ln(I)$ vs t, the H_v light scattering patterns cannot be observed except as an indistinct small spot which is an artifact due to reflection of the incident beam. Furthermore, a very weak broad overlapped X-ray diffraction intensity distribution from the (101) and (10$\bar{1}$) planes was observed by X-ray diffraction at about 100–120 min corresponding to the end of the linear portion of $\ln(I)$ vs time for 5% w/w solutions with the 50/50 compositions. Such diffraction intensity was also observed for gels with the 70/30 compositions at about 200–220 min. The appearance of such diffraction intensity indicating gelation/crystallization means that the straight line in the $\ln(I)$ vs t plot does not reflect the initial stage of pure spinodal decomposition.

With increasing time, the plot of $\ln(I)$ vs t deviates from the straight line and the corresponding X-type pattern under the H_v polarization condition becomes more distinct. In the present work, we must emphasize that this behavior is independent of the characteristics of the later stage of the spinodal decomposition as pointed out by Langer et al.[17] The X-type pattern indicates the existence of rodlike textures, the optical axis being oriented parallel or perpendicular to the rod axis.[20] The formation of rods is probably associated with the further development of gelation/crystallization in the polymer-rich phase. Thus, the deviation from the straight line in the $\ln(I)$ vs t plot is quite different from the later stage of phase separation as reported for polymer blends.[10] That is, in polymer blend systems, the further growth of concentration fluctuations associated with uphill diffusion is significant in the later stage of the spinodal decomposition and finally the concentration profile becomes similar to that of nucleation growth. In the present PVA solutions, however, such a further growth of concentraion fluctuations is suppressed because of immobilization of the PVA chains owing to crystallization.

To check for such a quasi-spinodal decomposition of the PVA solutions, the values of $R(q)$ were plotted as a function of q for a 1% w/w solution with the 50/50 composition at various temperatures. Figure 7 shows the result. The maximum relaxation rate $R(q_m)$ increases from 9×10^{-5} to 22×10^{-5} s^{-1} and the value of the wavenumber,

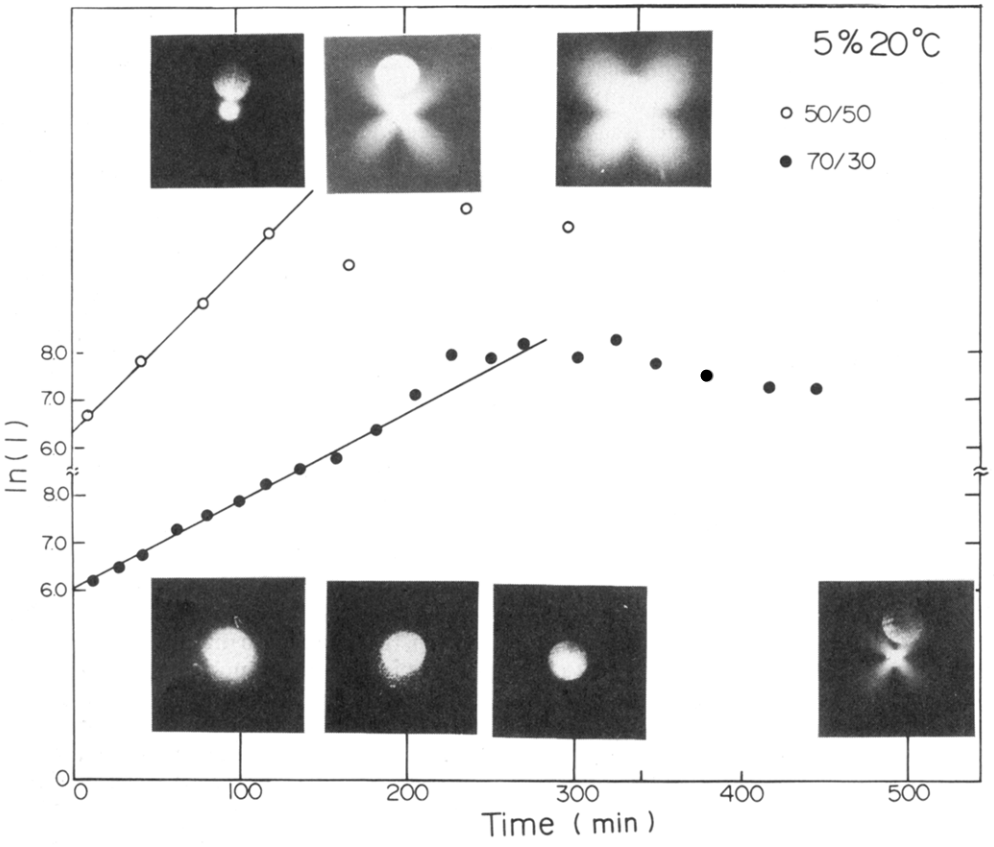

Figure 5. Change of $\ln(I)$ at $\theta = 90°$ and H_v light scattering patterns with time measured for 5% w/w solutions with the 50/50 and 70/30 composition at 20 °C.

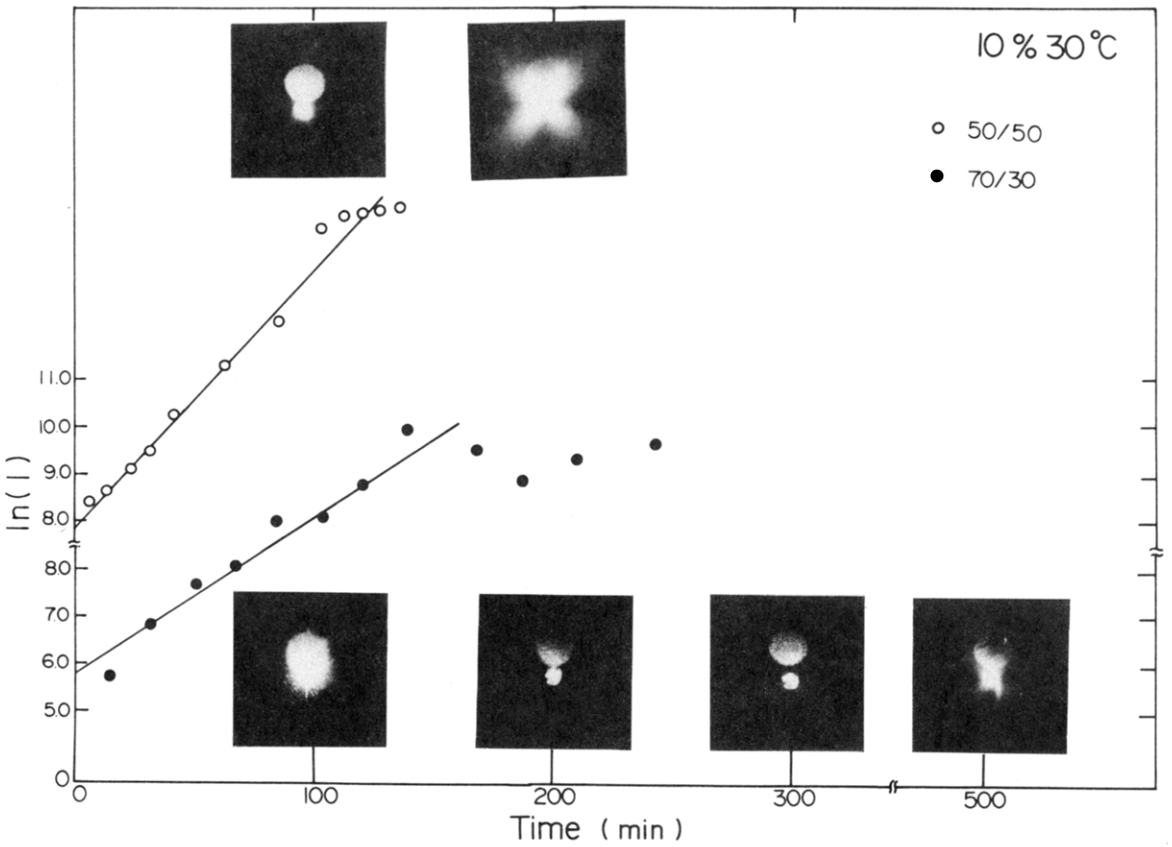

Figure 6. Change of ln(I) at $\theta = 90°$ and H_v light scattering patterns with time measured for 10% w/w solutions with the 50/50 and 70/30 compositions at 30 °C.

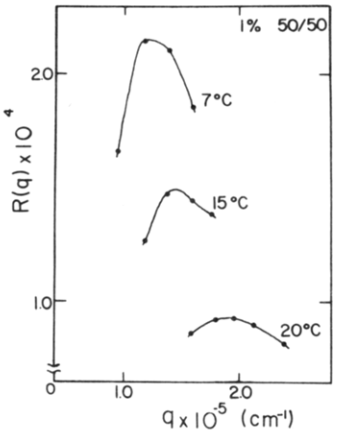

Figure 7. Variation of growth rate $R(q)$ of spinodal decomposition with q measured for 1% w/w solution with the 50/50 composition at the indicated temperatures.

q_m, of the spinodal decomposition fluctuation shifts toward the scattering center with decreasing temperature. This behavior is quite different from the formulation concerning spinodal decomposition of polymer solution proposed by van Aartsen.[9] According to his theory, the wavenumber q_m can be written as

$$q_m = \frac{1}{r_g}\left\{\frac{3|T_s - T|}{T_s}\right\}^{1/2} \tag{4}$$

where T and T_s are the experimental and spinodal temperatures, respectively, and r_g coresponds to the mean radius of gyration. Equation 4 means that q_m increases with increasing difference $(T_s - T)$ between experimental temperature, T, and spinodal temperature, T_s, if a range of molecular interaction associated with the mean radius of gyration, r_g, is independent of temperature, based on the concept of Debye.[21] In addition to such a result in this paper, the value of q_m reported for aqueous solutions of PVA by Komatsu et al.[6] was almost independent of $(T_s - T)$, indicating an inconsistency with the theory of van Aartsen.[9] If r_g is independent of temperature as discussed above, the two results together indicate that the phase separation of PVA solutions cannot be described by the linearized theory of the spinodal decomposition which has been applied to amorphous polymer solutions.[9]

However, van Aartsen pointed out that the value of r_g depends on the thermodynamic quality of the solvent and through this on temperature, on the molecular weight of the polymer, and most probably, on the concentration. To check whether the mean radius of gyration is independent of temperature, an attempt was made to estimate the value of r_g at a given temperature by using the following relationship:[22]

$$R_H(q) = \frac{4\pi^2}{\lambda^4}\frac{\left[\left(\frac{C}{\mu}\right)\left(\frac{\partial\mu}{\partial c}\right)\right]^2\left[1 - \frac{1}{3}r_g q^2\right]}{C\left[\left(\frac{\partial}{\partial c}\right)\left(\frac{P}{kT}\right)\right]} \tag{5}$$

where $R_H(q)$ is the Rayleigh ratio, C is the concentration of polymer in g/cm^3, μ is the index of refraction, P is the osmotic pressure, and k is Boltzmann's constant. Equation 5 is suitable for determining r_g at a given concentration by plotting $R_H(q)$ against q^2.

Before discussion of the gel structures, it was necessary to carry out measurements of $R_H(q)$ vs q^2 for the 0.1% w/w solutions. This is due to the fact that a very weak X-type pattern under the H_v polarization condition was observed even for gel prepared from 1% w/w solution, corresponding to the lowest concentration to form a gel. Accordingly, it is evident that application of eq 5 to optically anisotropic systems is unfavorable.

Figure 8 shows an example of plots of $R_H(q)$ vs q^2 for the 0.1% w/w solutions with the 50/50 and 70/30 com-

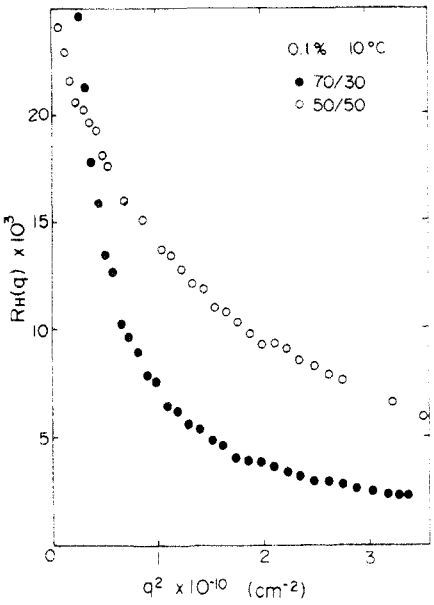

Figure 8. Rayleigh ratio $R_H(q)$ against q^2 measured for the 0.1% w/w solutions at the indicated temperatures.

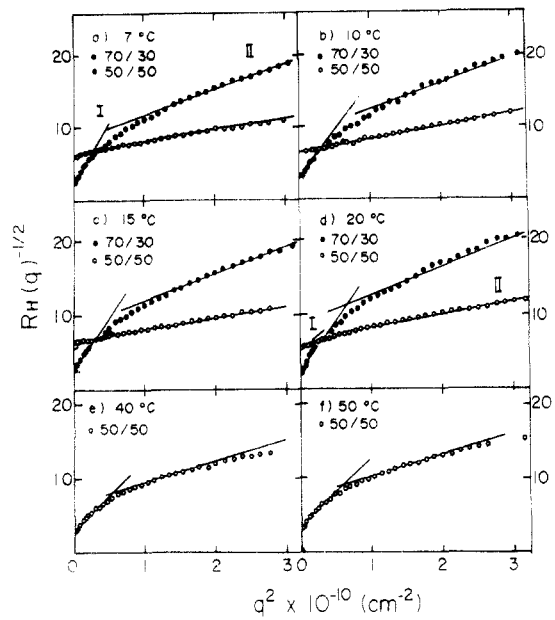

Figure 9. Plot of $R_H(q)^{-1/2}$ against q^2 measured for the 0.1% w/w solutions at the indicated temperatures.

positions measured at 10 °C. Before the measurements under the V_v polarization condition were carried out, the solution was stored for 2 weeks to ensure the equilibrium state at the experimental temperature. Actually, the scattered intensity measured for the given systems at fixed q increased slightly with time but was independent of time after a week.

As can be seen in this figure, however, the plot of $R_H(q)$ for both compositions shows strong curvature with q^2. Such a marked deviation from the straight line which is usually observed for polymer solutions can probably be attributed to the characteristics of PVA solutions, and it implies that for this system Zimm plots cannot be used to obtain the weight-average molecular weight of PVA by elastic light scattering.[23] However, using dilute aqueous PVA solution at a temperature of 80 °C, Matsuo and Inagaki were able to avoid the deviation from linearity in the Zimm plots,[24] presumably because the PVA molecules exist as isolated random coils at this temperature. If this is so, the curvature of the $R_H(q)$ vs q^2 plots at room temperature may be due to the fact that the PVA molecules are not isolated random coils but form superstructures with different sizes.

It can further be seen from Figure 8 that for the 70/30 composition $R_H(q)$ decreases drastically with q^2 and eventually becomes more or less constant. This means that the PVA chain characteristics are affected by the composition of solvent and is consistent with the phase separation behavior described above. Here a question arises as to whether the deviation from a linear relationship can be attributed to the effect of random orientational fluctuation and the fluctuation of optical anisotropy. To check these effects, the corresponding measurements were carried out for the V_H polarization condition, and these effects were found to be negligible, since the scattered intensity was almost zero. Thus, the curvature in the plots in Figure 8 can be expected if there exist several structures with different sizes in PVA solutions with 0.1% w/w concentration. If this is the case, each curve can be classified into several apparent straight lines, and hypothetical values of r_g can be determined from the slope and the intercept of the lines. However, such a procedure is questionable because the scattered intensity close to q = 0 contains unfavorable factors such as multiple scattering.

To confirm the above concept by another method, the correlation distance, a, is estimated at a given temperature by the following relationship:

$$R_H(q)^{-1/2} = (8\pi^2\langle\eta^2\rangle a^2)^{-1/2}(1 + a^2q^2) \qquad (6)$$

where $\langle\eta^2\rangle$ is the mean square fluctuation in average polarizability. Equation 6 can be easily derived by assuming that the correlation function in average polarizability can be approximated as $\exp(-r/a)$. The derivation of eq 6 is described in the Appendix. The 0.1% w/w solutions for the 50/50 and 70/30 compositions were employed to allow the assumption that the correlation distance is proportional to the mean radius of gyration.

Figure 9 shows the relationship between $R_H(q)^{-1/2}$ and q^2. Most of the plots show some curvature but a linear relationship is obtained at temperatures ≤ 15 °C for the 50/50 composition. The abnormal nonlinear behavior is thought to be due to the characteristics of PVA solutions as mentioned before. The plots for the 50/50 composition show a linear relationship at temperatures ≤ 15 °C, as has been observed generally for polymer dilute solutions and colloidal suspensions, but the plots tend to deviate from the linear relationship with increasing temperature. In contrast, for the 70/30 composition, the plot shows a curve in the temperature range mentioned. It should be noted that the plot of $R_H(q)$ vs q^2 in Figure 8 shows a curve in spite of the linear relation of the plot of $R_H(q)^{-1/2}$ vs q^2 for the 50/50 composition at temperatures ≤ 15 °C. This is essentially due to the different physical meaning of eqs 5 and 6. If the 0.1% w/w concentration is a dilute system for PVA chains, the correlation distance, a, is related to the particle (domain) size. In contrast, if the concentration is thought to be a concentrated system, a is not simply related to the size of the structural unit but depends upon both interparticle and intraparticle distance.[25-26] Except for the results of the 50/50 composition measured at 7, 10, and 15 °C, the correlation distance cannot be defined clearly. In any case, if each curve in Figure 9 is assumed to consist of two kinds of correlation distances reflecting structural parameters such as different domain sizes, the curve can be classified into two straight lines, I and II, approximately. The correlation distance obtained on the basis of the above concept is listed in Table II. The results indicate that the correlation distance, a, is also independent of temperatures ≤ 20 °C.[27]

On the basis of the information of the 0.1% w/w solution, plots of $R_H(q)^{-1/2}$ vs q^2 for the gels prepared from 2% w/w

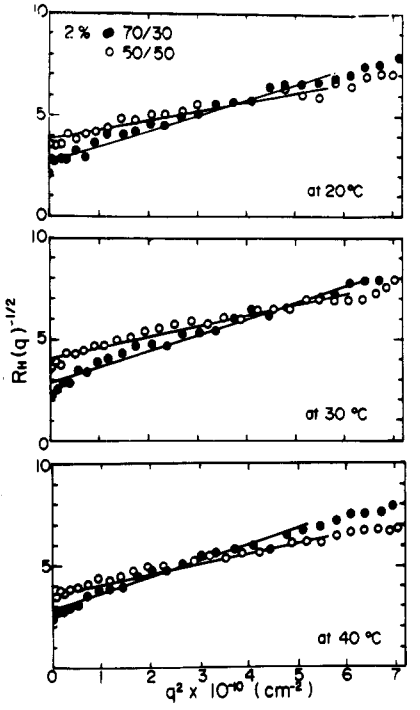

Figure 10. Plot of $R_H(q)^{-1/2}$ against q^2 measured for gels prepared from the 2% w/w solutions at the indicated temperatures.

Table II. Temperature Dependence of Correlation Distance (Å) in the 0.1% w/w PVA Solutions for the 50/50 and 70/30 Compositions

	temp (°C)					
comp	7	10	15	20	40	50
50/50				I 809	2520	2320
	510	526	526	II 518	740	749
70/30	I 2490	2390	2720	2520		
	II 689	682	686	701		

Table III. Temperature Dependence of Correlation Distance (Å) in the 2.0% w/w PVA Solutions (Gels) for the 50/50 and 70/30 Compositions

	temp (°C)		
comp	20	30	40
50/50	351	350	340
70/30	513	510	509

solutions were shown in Figure 10. Measurements were done after storing for 2 weeks to ensure the equilibrium state. As discussed before, a very weak X-type scattered intensity was observed under the H_v polarization condition. However, the scattered intensity under the V_H polarization condition detected by the photomultiplier was much weaker than that under the V_v polarization condition. Furthermore, it was confirmed that the scattering pattern under the V_v polarization condition is almost circular. In this case, eq 6 can be constructed approximately by neglecting the effect of V_H scattered intensity.

As can be seen in Figure 10, the plots for the 50/50 and 70/30 compositions show a linear relationship up to larger values of q^2, regardless of temperature < 40 °C. Because of the concentrated system, the correlation distance, a, is not simply related to the size of the structural unit, dependent upon both interparticle and intraparticle distance. Even so, it may be noted that each curve indicates the existence of one correlation distance. The correlation distance, a, obtained by using eq 6, is listed in Table III. The values are independent of temperature in the given range but dependent upon the composition. Judging from the results in Tables II and III, it may be concluded that if the correlation distance, a, is related to the domain size even in this gel system, the size of the domains becomes smaller and more uniform. This is thought to be due to the fact that an increase in concentration of solution plays an important role in forming gels with uniform structures because of an increase in packing density of PVA molecules. Anyway, it may be emphasized that the correlation distance is independent of temperature in gels. Thus, the shift of $R(q)$ to lower values of q on increasing the difference $(T - T_s)$ shown in Figure 7 justifies the earlier conclusion that neither the linearized theory of the spinodal decomposition proposed by van Aartsen[9] nor the theory of Cahn is applicable to the present system.

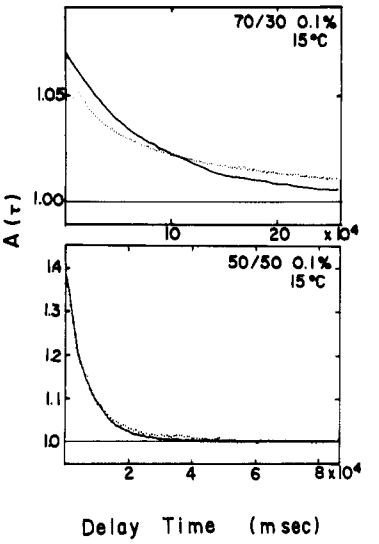

Figure 11. Autocorrelation function $A(\tau)$ against delay time τ at 15 °C for the 0.1% w/w solutions with the 70/30 and 50/50 compositions.

To obtain more detailed information on the characteristics of the PVA solutions and gels, inelastic light scattering measurements were carried out. The evaluation of the data was done by the histogram and cumulative methods for determining the distribution of decay rate Γ from the observed correlation function.

Figure 11 shows the autocorrelation function $A(\tau)$ at 15 °C plotted against delay time τ for the 0.1% w/w solutions with the 70/30 and 50/50 compositions. The sample preparation was done according to the same process as the measurements in Figure 9. The measurements were done at $\theta = 90°$. The full curves are also autocorrelation functions recalculated from the histogram. All the calculations were carried out by assuming a unimodal system. The recalculated curves are in good agreement with the experimental results for the 50/50 composition. In contrast, the curves are in poor agreement with the experimental results for the 70/30 composition. This is probably related to the very slow decrement of autocorrelation function $A(\tau)$ as well as the small value of $A(\tau)$ at $q^2 = 0$. The adoption of the unimodal system was decided on the basis of a preliminary finding that, although a bimodal-like or a trimodal-like distribution gives a complicated histogram with one or two small peaks in addition to the main peak of the Γ distribution, the autocorrelation functions recalculated from the complicated histogram are almost equal to those in Figure 11. The histogram calculated by a bimodal-like or a trimodal-like distribution is surely important to analyze domains having sizes depending on the concentration and the composition of the solvent. Unfortunately, in this system, no statistical relationship for domain size could be recognized from the complicated histogram calculated by assuming a bimodal-like or a trimodal-like distribution. This is probably due to the broad molecular weight distribution of PVA with $\bar{M}_w/\bar{M}_n = 3.20$.

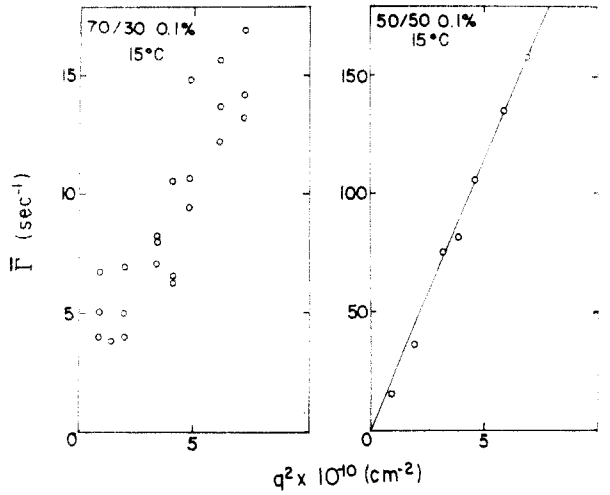

Figure 12. q^2 dependence of $\bar{\Gamma}$ for the 0.1% w/w solution with the 70/30 and 50/50 compositions measured at 15 °C.

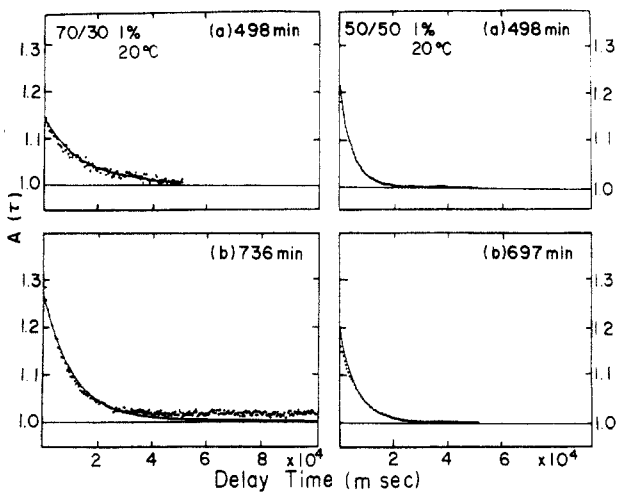

Figure 13. Autocorrelation function $A(\tau)$ against delay time τ at 20 °C for the 1% w/w solutions with 70/30 and 50/50 compositions measured at the indicated times.

Figure 12 shows the q^2 dependence of $\bar{\Gamma}$ calculated by the cumulative method for the 50/50 and 70/30 compositions at 15 °C. The plots of $\bar{\Gamma}$ vs q^2 yield a linear relationship for the 50/50 composition, consistent with the definition of the diffusion coefficient D by $D = \bar{\Gamma}/q^2$ based on the second law of Fick. In contrast, the plots for the 70/30 composition are scattered and the values of $\bar{\Gamma}$ are much lower than those for the 50/50 composition. This phenomenon supports the results in Figure 9 and indicates that there is a correlation distance associated with small fluctuation of size distribution in the solution with the 50/50 composition, while there are two or three statistical structures with different sizes in the solution with the 70/30 composition.

This analysis for the 70/30 composition, however, is only hypothetical, since the autocorrelation function recalculated from its histogram is in poor agreement with the exponential plots even at the initial stage of the delay time shown in Figure 10. This ambiguity is due to the much slower decrement as well as the much smaller values of $A(\tau)$ around $q^2 = 0$ in comparison with the profile of the 50/50 composition.

Figure 13 shows the autocorrelation function $A(\tau)$ at 20 °C plotted against delay time τ for the 1% w/w solutions with the 70/30 and 50/50 compositions by assuming that the equilibrium state in solution is maintained during the photon counting period of 5 min. These figures correspond to data obtained at two different times after the start of the experiment. Incidentally, the sample preparation used

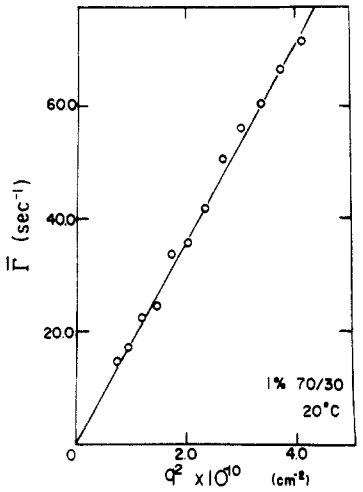

Figure 14. q^2 dependence of $\bar{\Gamma}$ for the 1% w/w solution with the 70/30 composition measured at 20 °C.

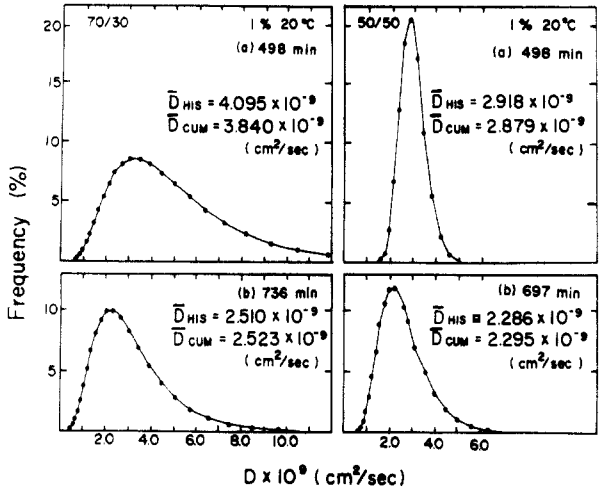

Figure 15. Distribution of the diffusion coefficient, D, calculated from the histogram method for the 1% w/w solutions with the 70/30 and 50/50 compositions measured at 20 °C.

for the measurement of inelastic light scattering is the same as that used for the measurement of ln(I) vs time by elastic light scattering shown in Figures 1 and 2. The recalculation functions (full curve) from the histogram method are in good agreement with the experimental results.

Figure 14 shows the q^2 dependence of $\bar{\Gamma}$ calculated by the cumulative method for the 1% w/w solution with the 70/30 composition at 20 °C. The measurements were done after 498 min by considering that the change in $\bar{\Gamma}$ is too slow to allow measurement of the q^2 dependence. As shown in Figure 14, plots of $\bar{\Gamma}$ vs q^2 yielded a linear relationship, thus assuring the definition of D by $\bar{\Gamma} = Dq^2$, in spite of the scattered plots for the 0.1% w/w solution as shown in Figure 11. This phenomenon indicates that with increasing concentration the resultant gels form a concentrated heterogeneous system with small fluctuation of domain size. This is in good agreement with the results in Figure 10. The linearity was also confirmed after 222 min for the 5% w/w solutions with the 50/50 and 70/30 compositions at 20 °C in spite for the scattering from anisotropic rods showing azimuthal angular dependence of the very weak scattered intensity under the V_v polarization condition.

Figure 15 shows distributions of the diffusion coefficient, D, calculated by the histogram method. In each frame, the mean value ($\bar{D}_{HIS}$) estimated as the center of gravity of the distribution curve and the value of $\bar{D}_{CUM}$ calculated by the cumulative method are listed together. It is seen that the values of $\bar{D}_{HIS}$ is in good agreement with that of

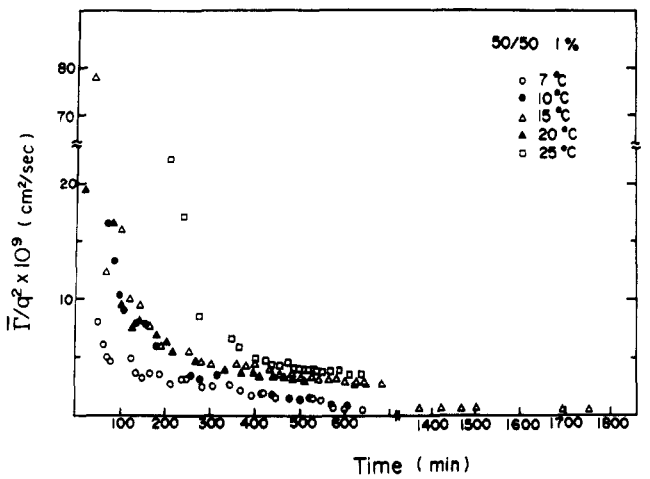

Figure 16. Time dependence of $\bar{\Gamma}/q^2$ at $\theta = 90°$ for the 1% w/w solution with the 50/50 composition measured at the indicated temperatures.

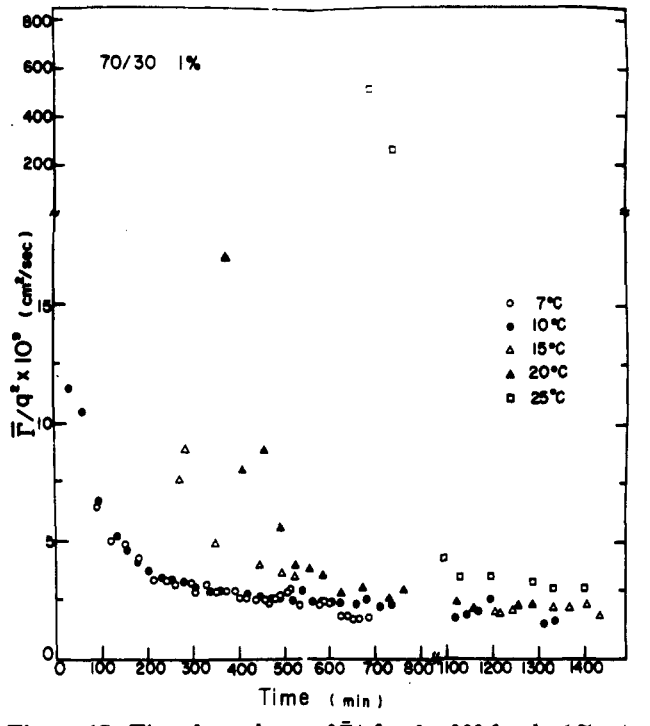

Figure 17. Time dependence of $\bar{\Gamma}/q^2$ at $\theta = 90°$ for the 1% w/w solution with the 70/30 composition measured at the indicated temperatures.

$\bar{D}_{CUM}$, indicating reliability of the distribution of D. The distribution of D for the 50/50 composition is sharper than that for the 70/30 composition, and the values of $\bar{D}_{HIS}$ and $\bar{D}_{CUM}$ for the 50/50 composition are lower. These phenomena imply that the gelation mode at the 50/50 composition is simpler than that at the 70/30 composition and the process of gel formation is faster. The analysis, however, still remains unresolved. Thus, it turns out that the gelation of PVA solution is sensitive to the composition of the cosolvent. The same tendency was also confirmed for other concentrations.

As discussed before, it was very difficult to check the linearity of the plot of $\bar{\Gamma}$ vs q^2 in the time scale < 498 min for the 50/50 and 70/30 compositions. Accordingly, the gelation mechanism is discussed in terms of the time dependence of $\bar{\Gamma}/q^2$ at $\theta = 90°$ using a cumulative method instead of the diffusion coefficient $\bar{D}_{CUM}$ or $\bar{D}_{HIS}$. Figures 16 and 17 show the results at the indicated temperatures measured for the 1% w/w solutions with the 50/50 and 70/30 compositions, respectively. The calculations of $\bar{\Gamma}$ were carried out by the cumulative method. The value of $\bar{\Gamma}/q^2$ decreases rapidly at the shorter time scale and then

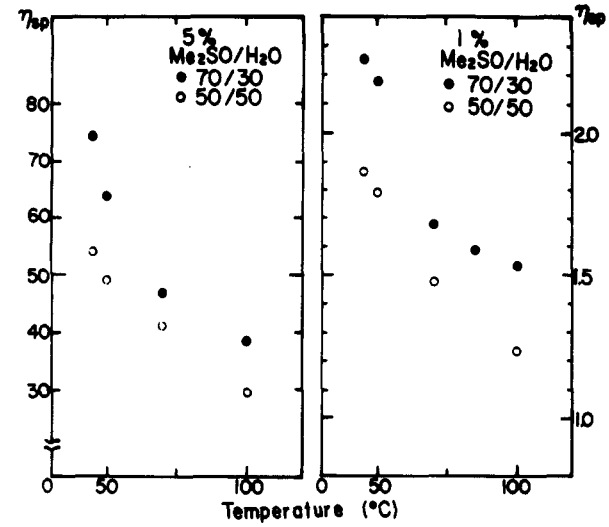

Figure 18. Specific viscosity η_{sp} against temperature measured for the 5 and 1% w/w solutions.

tends to level off. Furthermore, the drastic decrease in $\bar{\Gamma}/q^2$ at temperatures > T_s shifts to a much longer time scale. Interestingly, in the present analysis, the critical time corresponding to the leveling-off point of the $\bar{\Gamma}/q^2$ plot is almost equal to the time associated with the deviation from the linear relationship of $\ln(I)$ vs t, shown in Figures 1 and 2. In addition to the appearance of the X-ray diffraction intensity from the (101) and (10$\bar{1}$) planes and the H_v scattering pattern discussed before, the observed time dependence of $\bar{\Gamma}$ also supports the interpretation that the linearity in Figures 1 and 2 is attributable to a quasi-spinodal decomposition corresponding to the simultaneous occurrence of spinodal decomposition and gelation in the PVA solutions. If the linearity was due to pure spinodal decomposition, the diffusion coefficient $\bar{D}_{CUM}$ (or $\bar{D}_{HIS}$) estimated by inelastic light scattering would be expected to have a constant value independent of time. Accordingly, it follows that the observed time dependence is not consistent with the linearized spinodal decomposition theory[15] which assumes time independence of $D_{app} = -D_c(\partial^2 f/\partial c^2)$.

Figure 18 shows a plot of specific viscosity η_{sp} against temperature under the indicated conditions. The viscosity at the 70/30 composition is higher than that at the 50/50 composition. This implies that the cosolvent with the 50/50 composition is poorer for PVA molecules than that with the 70/30 composition and that the size or spatial extension of the polymer chains in solution has a significant effect on the development of spinodal decomposition and gelation. The result in Figure 18 indicates that intramolecular coupling entanglements play an important role in promoting spinodal decomposition and gelation rather than intermolecular decomposition. The reason for this behavior still remains unresolved.

Here it should be noted that according to the preliminary experiments[5] the maximum draw ratio of the dried PVA gel films could be realized when the gel was prepared by quenching the solution with the 70/30 composition at −50 °C. It was found that under these conditions, the crystallinity of the undrawn film is the lowest and no superstructure could be observed by small-angle light scattering under H_v polarization. This indicates that spinodal decomposition hampers drawability of the resultant dried gel films and that the quenching plays an important role in arresting the progression of spinodal decomposition. The occurrence of the lowest crystallinity is thought to be due to the fact that the rapid gelation hampers the promotion of crystallization. To check the validity of this concept, two kinds of gels were prepared

Table IV. Characteristics of Dried Gel Films Prepared by Gelation/Crystallization[a]

temp of gelation/ crystallization (°C)	comp	undrawn film crystallinity (%)	at maximum draw ratio		
			storage modulus (GPa)	crystallinity (%)	birefringence (×10⁻³)
−50	50/50	12	27 (λ = 11)	24	42
	70/30	10	29 (λ = 12.5)	27	45
+20	50/50	28	15 (λ = 8)	36	30
	70/30	21	18 (λ = 9)	39	32

[a] The crystallinity was calculated by assuming densities of the crystal and amorphous phases to be 1.345 and 1.269, respectively.[28]

from the 5% w/w solutions with the 70/30 and 50/50 compositions by the same method as employed for preparation of the specimens for measuring ln(I) vs t in Figure 5. After 100 min, the two gels were quenched at −50 °C to stop the progression of spinodal decomposition, and subsequently the cosolvents with the 70/30 and 50/50 compositions were evaporated from each gel to −50 °C. The crystallinities of the resultant dried gel films obtained for the 70/30 composition were in the range 11–13%, which is lower than in the range 17–20% of the films obtained for the 50/50 composition. The elongation was done under nitrogen at 125 °C. This temperature was closen to avoid dehydration. The maximum draw ratio of the film prepared from the former composition reached 11.5, which is slightly higher than the values, 9–10, obtained for the latter composition.

Returning to Figure 5, it may be noted that the plot of ln(I) vs t deviates from linearity beyond 120 min for the solution with the 50/50 composition, while they were linear up to 200 min for the solution with the 70/30 composition. This means that 100 min corresponds to the final period of the initial stage of the quasi-spinodal decomposition for the solution with the 50/50 composition, while for the latter solution 100 min still corresponds to the initial stage of the quasi-spinodal decomposition. This is due to the faster progression of the quasi-spinodal decomposition of the former solution than for the latter solution. Accordingly, it may be concluded that the quasi-spinodal decomposition hampers facile drawability of PVA dried gel films.

To facilitate understanding of the above concept, the mechanical properties were investigated using films prepared by gelation/crystallization from 5% w/w solutions with the 50/50 and 70/30 compositions. The temperatures for the gelation/crystallization were set at −50 and 20 °C. The gels prepared at −50 °C were vacuum-dried at −50 °C as soon as possible to suppress the spinodal decomposition as well as an increase in crystallinity during solvent evaporation. The resultant films were transparent. In contrast, the gels prepared at 20 °C were stored for a week under tension to ensure simultaneous occurrence of gelation and spinodal decomposition during solvent evaporation and then dried under ambient conditions. The resultant films were whiter than those prepared at −50 °C, and this was the most marked for the 50/50 composition. The specimen placed in an oven at 125 °C was elongated manually to the desired draw ratio under a nitrogen flow to avoid dehydration.

Table III shows the storage modulus (Young's modulus) at 20 °C, crystallinity, and birefringence. The storage modulus was measured at 10 Hz at 20 °C by using an Iwamoto viscoelastic spectrometer (VES-F). The length of the specimen between the jaws was 40 mm and the width was 1.5 mm. The crystallinity was lowest when the solution with the 70/30 composition was quenched and subsequently vacuum-dried at −50 °C. The draw ratio (λ) and storage modulus of the film reached maximum values. The results in Table IV support the concept that the rapid gelation suppresses the spinodal decomposition which hampers facile drawability of the resultant films.

Concluding Remarks

In the present investigation, phase separation from PVA solutions in dimethyl sulfoxide/water mixtures has been studied by elastic and inelastic light scattering. The principal results are as follows: The plot of the logarithm of the scattered intensity against time yielded a straight line in the initial stage of phase separation and deviated from the linearity in the later stage. At the later stage, an X-type pattern could be observed under the H_v polarization condition, indicating the existence of a rodlike texture, the optical axes being oriented parallel or perpendicular with respect to the rod axis. On the other hand, the values of $\bar{\Gamma}/q^2$ measured by inelastic light scattering decreased drastically and tended to level off at longer times. These results have been interpreted as indicating that the phase separation process consists of the simultaneous occurrence of spinodal decomposition and gelation. Furthermore, the results provide a basis for relating the drawability of dried PVA films prepared from Me_2SO/H_2O solutions to the characteristics of molecular chains in solution.

Acknowledgment. We thank Prof. Tsunashima, Chemical Institute of Kyoto University, for valuable comments and suggestions for measuring autocorrelation functions. We are also grateful to Prof. Manley, Department of Chemistry, Pulp and Paper Building, McGill University, for his kind help with linguistic revision of the manuscript. We are indebted Prof. Iwai, Faculty of Science, Nara Women's University, for measuring $\bar{M}_w$ and $\bar{M}_n$ of the PVA sample by gel permeation chromatography.

Appendix

According to the Debye–Bueche theory,[29] the Rayleigh ratio $R_H(q)$ for an isotropic system is given by

$$R_H(q) = \langle \eta^2 \rangle \int_0^\infty \gamma(r) \frac{\sin(qr)}{qr} r^2 \, dr \qquad \text{(A-1)}$$

where $\gamma(r)$ is a correlation function. If $\gamma(r)$ is given by $\exp(-r/a)$, eq A-1 deduces to eq 6.

References and Notes

(1) Sakurada, I.; Nukushina, Y.; Ito, T. *J. Polym. Sci.* **1962**, *57*, 651.
(2) Sakurada, I.; Ito, T.; Nakamae, K. *J. Polym. Sci.* **1966**, *15*, 75.
(3) Hyon, S. H.; Chu, W. I.; Ikada, Y. *Rep. Poval Committee* **1986**, *89*, 1.
(4) Friedberg, F.; Brown, W.; Henley, D.; Öhman, J. *Makromol. Chem.* **1983**, *66*, 168.
(5) Sawatari, C.; Yanagida, N.; Yamamoto, Y.; Matsuo, M. *Polymer* **1993**, *34*, 956.
(6) Komatsu, M.; Inoue, T.; Miyasaka, K. *J. Polym. Sci.* **1986**, *24*, 303.
(7) Coniglio, A.; Stanly, H. E.; Klein, W. *Phys. Rev. Lett.* **1979**, *42*, 518.
(8) Fang, L.; Brown, W. *Macromolecules* **1990**, *23*, 3284.
(9) van Aartsen, J. J. *Eur. Polym. J.* **1970**, *6*, 919.
(10) Nishi, T. *J. Macromol. Sci., Phys.* **1980**, *B17* (3), 517.
(11) Berne, B. J.; Pecora, R. *Dynamic Light Scattering*; John Wiley and Sons, Inc.: New York, 1976.
(12) Chu, B. *Laser Light Scattering*; Academic Press: New York, 1974.
(13) Koppel, D. E. *J. Chem. Phys.* **1972**, *57*, 4814.

(14) Nemoto, N.; Tsunashima, Y.; Kurata, M. *Polym. J.* **1981**, *13*, 827.
(15) Cahn, J. W. *J. Chem. Phys.* **1965**, *42*, 93.
(16) Cahn, J. W.; Hilliard, J. E. *J. Chem. Phys.* **1958**, *28*, 258.
(17) Langer, J. S.; Bar-on, M.; Miller, H. S. *Phys. Rev. A* **1975**, *11*, 1417.
(18) Kawasaki, K.; Ohta, T. *Prog. Theor. Phys.* **1978**, *59*, 362.
(19) Hung, J. S.; Goldburg, W. I.; Bjer Kaas, A. W. *Phys. Rev. Lett.* **1974**, *32*, 921.
(20) Rhodes, M. B.; Stein, R. S. *J. Polym. Sci., Part A-2* **1969**, *7*, 1539.
(21) Debye, P. *J. Chem. Phys.* **1959**, *31*, 680.
(22) Debye, P.; Woermann, D. *J. Chem. Phys.* **1962**, *36*, 1803.
(23) The range of eq 5 is limited at only scattering angles close to $q = 0$ and is related to Zimm plots by using $1/(1 - x) = 1 + x$ ($x \ll 1$). Even so, plots of $R_H(q)$ vs q^2 in eq 5 actually have given a linear relationship at relatively high values of q for most polymers, and consequently Zimm plots have been useful. In other words, if plots of eq 5 deviate from a straight line, the Zimm plots cannot be used.
(24) Matsuo, T.; Inagaki, H. *Makromol. Chem.* **1962**, *55*, 150.
(25) Debye, P.; Anderson, H. R.; Brumberger, H. *J. Appl. Phys.* **1957**, *28*, 679.
(26) Khambatta, F. B.; Warner, F.; Russell, T.; Stein, R. S. *J. Polym. Sci., Polym. Phys. Ed.* **1976**, *14*, 1391.
(27) Plots of the 50/50 composition at 20 °C can be classified into two straight lines, I and II, but the plots for the most part can be represented by line II. The value of a estimated by line II is 518 Å, which suggests a temperature independence of the correlation distance at <20 °C.
(28) Sakurada, I.; Nukushina, K.; Sone, Y. *Kobunshi Kagaku* **1955**, *12*, 506.
(29) Debye, P.; Bueche, A. M. *J. Appl. Phys.* **1949**, *20*, 518.